Fig. 5 shows the measured amplitude and phase characteristics of the high-power amplifier under test. The two-tone average output powers of fundamental, IM3, and IM5 are plotted in Fig. 5(a). The measured relative phases are plotted in Fig. 5(b). The first measurement point of fundamental is set to zero phase and the others are calculated to have relative values. The measured phases of IM3 and IM5 vary rapidly as the power level approaches saturation.

IV. Conclusion

To adequately consider the memory effect for high-power amplifiers, we have presented a new accurate method for measuring two-tone transfer characteristics. We measured the characteristics of a multistage high-power amplifier with a 500-W power output and 44.5-dB gain. We have used a trustworthy reference IM generator at a very low frequency. The two-tone harmonic balance simulation shows the accuracy of the relative phase of the reference IM generator. The complete measurement setup and sequence have been described.

We measured the relative phases of fundamental, IM3, and IM5. The measured data of IM3 and IM5 are very smooth and continuous, and vary rapidly as the power level approaches the output power saturation. The measured two-tone transfer characteristics are very useful for the design of predistortion linearizer or nonlinear model extraction for high-power amplifiers.

References

[1] K. G. Gard, H. M. Gutierrez, and M. B. Steer, "Characterization of spectral regrowth in microwave amplifiers based on the nonlinear transformation of a complex Gaussian process," *IEEE Trans. Microwave Theory Tech.*, vol. 47, pp. 1059–1069, July 1999.

[2] Q. Wu, H. Xiao, and F. Li, "Linear RF power amplifier design for CDMA signals: A spectrum analysis approach," *Microwave J.*, pp. 22–40, Dec. 1998.

[3] C. J. Clark, G. Chrisikos, M. S. Muha, A. A. Moulthrop, and C. P. Silva, "Time-domain envelope measurement technique with application to wide-band power amplifier modeling," *IEEE Trans. Microwave Theory Tech.*, vol. 46, pp. 2531–2540, Dec. 1998.

[4] A. Leke and J. S. Kenny, "Behavioral modeling of narrowband microwave power amplifiers with applications in simulating spectral regrowth," in *IEEE MTT-S Microwave Symp. Dig.*, 1996, pp. 1385–1388.

[5] S. Chen, W. Panton, and R. Gilmore, "Effects of nonlinear distortion on CDMA communication systems," *IEEE Trans. Microwave Theory Tech.*, vol. 44, pp. 2743–2750, Dec. 1996.

[6] W. Bosch and G. Gatti, "Measurement and simulation of memory effects in predistortion linearizers," *IEEE Trans. Microwave Theory Tech.*, vol. 37, pp. 1885–1890, Dec. 1989.

[7] N. Suematsu, Y. Iyama, and O. Ishida, "Transfer characteristics of IM3 relative phase for a GaAs FET amplifier," *IEEE Trans. Microwave Theory Tech.*, vol. 45, pp. 2509–2514, Dec. 1997.

[8] S. A. Maas and D. Neilson, "Modeling MESFET's for intermodulation analysis of mixers and amplifiers," *IEEE Trans. Microwave Theory Tech.*, vol. 38, pp. 1964–1971, Dec. 1990.

[9] J. C. Pedro and J. Perez, "Accurate simulation of GaAs MESFET's intermodulation distortion using a new drain-source current model," *IEEE Trans. Microwave Theory Tech.*, vol. 42, pp. 25–33, Dec. 1997.

[10] T. M. Roh, Y. Kim, Y. Suh, and B. Kim, "A new simple extraction method for higher order components of channel current in GaAs MESFET," in *27th European Microwave Conf. Dig.*, Jerusalem, Israel, Sept. 1997, pp. 415–421.

Integration Equation Analysis on Resonant Frequencies and Quality Factors of Rectangular Dielectric Resonators

Shyh-Yeong Ke and Yuan-Tung Cheng

***Abstract*—In this paper, the resonance problem of rectangular dielectric resonators (DRs) is analyzed by using the spectral dyadic Green's function and volume integral-equation formulation. The rectangular dielectric body is replaced by a set of entire-domain polarized volume current basis, and Galerkin's moment method is used to solve the resonant frequency and quality factor of the rectangular DR. The effects of electrical and geometrical parameters on the resonance of the TE_{111} mode of isolated DRs are also presented. Additionally, the case of a rectangular DR with a ground plane is also discussed. Results are found to be in good agreement with the published experimental data.**

***Index Terms*—Dielectric resonators, method of moments.**

I. Introduction

Dielectric resonators (DRs) are extensively used for microwave circuit components such as filters and antennas [1], [2]. Recently, open rectangular DRs for use as radiation elements have received increasing attention due to their simplified mechanism and easy integration with microwave integrated circuits (MICs). Besides, the microwave components made of high-permittivity dielectric materials have the advantages of small size and temperature stability. In the DR filter or DR antenna design, the quality factor is a very important consideration since it accounts for the loss (dielectric and radiation losses) of a DR. Furthermore, accurate prediction of the DR's resonant frequency is of interest in the design of a narrow-band component. A number of studies for rigorously evaluating the resonant frequencies and quality factors of cylindrical or rectangular box-like DRs have been reported. The surface integral formulation [3], the least-square method [4], the mode-matching method [5], and the finite-difference time-domain method [6] have been successfully used to investigate the resonance problems of cylindrical DR structures. However, the exact numerical method for analyzing electromagnetic problems of a three-dimensional structure often takes much CPU time. This motivates this present study of using an accurate and efficient numerical method to analyze the resonance problems of open rectangular DR structures.

In this paper, the resonant frequencies and radiation Q factors of TE_{111} modes of open rectangular DRs are investigated by using a volume integral-equation solution. The spectral dyadic Green's functions and electric-field integral equations are derived and described in the Section II. A set of entire-domain volume current basis is presented for efficiently calculating the complex resonant frequencies of rectangular DRs. In Section III, numerical results are presented and discussed. Finally, conclusions are presented in Section IV.

II. Theory

A. Spectral Dyadic Green's Function and Integral-Equation Formulation

Fig. 1 shows the geometry of the rectangular DR under consideration. The rectangular DR is with a dimension of $2W \times 2L \times 2h$ and a

Manuscript received November 16, 1999. This work was supported by the National Science Council, R.O.C., under Grant NSC88-2213-E145-006.

The authors are with the Department of Electrical Engineering, Chinese Military Academy, Kaohsiung, Taiwan 830, R.O.C. (e-mail: syke@cc.cma.edu.tw).

Publisher Item Identifier S 0018-9480(01)01699-4.

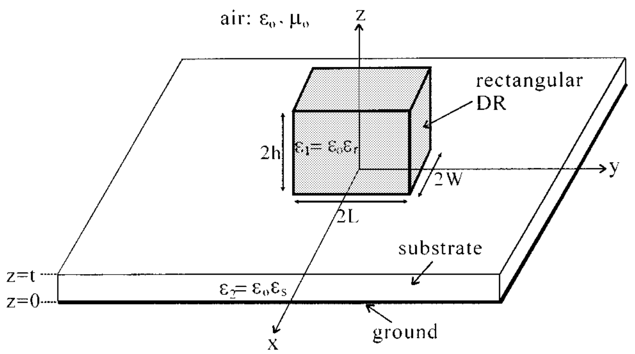

Fig. 1. Geometry of a rectangular DR on a grounded substrate.

relative permittivity of ε_r, and is located on a grounded substrate. The substrate has a thickness of t and a relative permittivity ε_s. Here, the substrate is assumed to be uniform and of infinite extension. The air is with permittivity ε_o and permeability μ_o. In the absence of the feed source, the electromagnetic problem of the DR with the permittivity $\varepsilon_1 = \varepsilon_o \varepsilon_r$ is equivalent to have the polarized current source (suppressing $e^{j\omega t}$ time dependence)

$$\vec{J}_{eq}(\vec{r}) = j\omega\varepsilon_o(\varepsilon_r - 1)\vec{E}(\vec{r}) \tag{1}$$

where $\vec{E}(\vec{r})$ is the total electric field, which consists of the incident electric field $\vec{E}^i(\vec{r})$ due to $\vec{J}_{eq}(\vec{r})$ and the scattering field $\vec{E}^s(\vec{r})$ due to the obstacle (the grounded substrate). The total electric field can be written as the integral equation

$$\vec{E}(\vec{r}) = k_o^2(\varepsilon_r - 1)\iiint_{V_d} \overline{\overline{G}}(\vec{r}, \vec{r}\,') \cdot \vec{E}(\vec{r}\,')\, dV(\vec{r}\,') \tag{2}$$

where $k_o = \omega\sqrt{\mu_o\varepsilon_o}$, V_d is the volume occupied by the rectangular DR and $\overline{\overline{G}}(\vec{r}, \vec{r}\,')$ denotes the dyadic Green's function, described by the following spectral expression [7]:

$$\overline{\overline{G}}(\vec{r}, \vec{r}\,') = \frac{-j}{8\pi^2 k_o^2}\int_{-\infty}^{\infty}\int_{-\infty}^{\infty} \overline{\overline{g}}(k_x, k_y, z, z') \cdot \frac{e^{jk_x(x-x')}e^{jk_y(y-y')}}{k_z}\, dk_x dk_y - \frac{\hat{z}\hat{z}}{k_o^2}\delta(\vec{r} - \vec{r}\,'). \tag{3}$$

In (3), $\overline{\overline{g}}(k_x, k_y; z, z')$ can be expressed in the following matrix form:

$$\overline{\overline{g}}(k_x, k_y; z, z') = \left[\overline{\overline{g}}_{\rm TE}^{(i)}(k_x, k_y) + \overline{\overline{g}}_{\rm TM}^{(i)}(k_x, k_y)\right]e^{-jk_z|z-z'|} + \left[R_{\rm TE}\,\overline{\overline{g}}_{\rm TE}^{(s)}(k_x, k_y) + R_{\rm TM}\,\overline{\overline{g}}_{\rm TM}^{(s)}(k_x, k_y)\right] \cdot e^{-jk_z(z+z')} \tag{4}$$

with

$$\overline{\overline{g}}_{\rm TE}^{(i)}(k_x, k_y) = \overline{\overline{g}}_{\rm TE}^{(s)}(k_x, k_y) = \begin{bmatrix} k_o^2k_y^2/\beta^2 & -k_xk_yk_o^2/\beta^2 & 0 \\ -k_xk_yk_o^2/\beta^2 & k_x^2k_o^2/\beta^2 & 0 \\ 0 & 0 & 0 \end{bmatrix} \tag{5a}$$

$$\overline{\overline{g}}_{\rm TM}^{(i)}(k_x, k_y) = \begin{bmatrix} k_x^2k_z^2/\beta^2 & k_xk_yk_z^2/\beta^2 & k_xk_{z\,-}^{\,+} \\ k_xk_yk_z^2/\beta^2 & k_y^2k_z^2/\beta^2 & k_yk_{z\,-}^{\,+} \\ k_xk_{z\,-}^{\,+} & k_yk_{z\,-}^{\,+} & \beta^2 \end{bmatrix} \tag{5b}$$

$$\overline{\overline{g}}_{\rm TM}^{(s)}(k_x, k_y) = \begin{bmatrix} -k_x^2k_z^2/\beta^2 & -k_xk_yk_z^2/\beta^2 & k_xk_z \\ -k_xk_yk_z^2/\beta^2 & -k_y^2k_z^2/\beta^2 & k_yk_z \\ -k_xk_z & -k_yk_z & \beta^2 \end{bmatrix} \tag{5c}$$

$$R_{\rm TE} = \frac{k_z\sin k_{zs}t + jk_{zs}\cos k_{zs}t}{k_z\sin k_{zs}t - jk_{zs}\cos k_{zs}t}\,e^{j2k_zt} \tag{5d}$$

$$R_{\rm TM} = \frac{\varepsilon_sk_z\cos k_{zs}t - jk_{zs}\sin k_{zs}t}{\varepsilon_sk_z\cos k_{zs}t + jk_{zs}\sin k_{zs}t}\,e^{j2k_zt} \tag{5e}$$

where

$$\beta^2 = k_x^2 + k_y^2$$
$$k_z = \sqrt{k_o^2 - \beta^2}$$
$$k_{zs} = \sqrt{\varepsilon_sk_o^2 - \beta^2}$$

and

$$k_{z\,-}^{\,+} = \begin{cases} k_z, & z > z' \\ -k_z, & z < z'. \end{cases}$$

The first term on the right-hand side of (4) is the Green's function for the rectangular DR in an unbounded medium. The second term on the right-hand side of (4) is the Green's function that accounts for the effect of the obstacle on the wave propagation. The leakage phenomenon of a dielectric material is caused by TE–TM wave coupling [8]. $R_{\rm TE}$ and $R_{\rm TM}$ are, respectively, the reflection coefficients of TE and TM waves incident upon the boundary $z = t$ from the air region to the substrate region.

B. Entire-Domain Basis and the Moment-Method Solution

This section describes the numerical method of calculating the electric-field integral equation in (2). The computation time is largely reduced by calculating the integral equation in a two-dimensional (k_x and k_y) space. First, a set of entire-domain volume current basis is utilized to expand the electric fields inside the rectangular DR. The advantage from choosing the entire-domain basis is its efficiency in the numerical calculation since few unknowns are to be determined. Here, the entire-domain basis functions based on the magnetic wall model are chosen to be

$$\begin{aligned} E_x(\vec{r}) &= \sum_{m=1}^{\infty}\sum_{n=1}^{\infty}\Big[\Big(I_{1,mn}^xe_{mn}^{(1)} + I_{2,mn}^xe_{mn}^{(2)} + I_{3,mn}^xe_{mn}^{(3)}\Big) \cdot \cos k_{z,mn}z + \Big(I_{4,mn}^xe_{mn}^{(1)} + I_{5,mn}^xe_{mn}^{(2)} + I_{6,mn}^xe_{mn}^{(3)}\Big) \cdot \sin k_{z,mn}z\Big] \\ &= \sum_{m=1}^{\infty}\sum_{n=1}^{\infty}\sum_{p=1}^{6} I_{p,mn}^xb_{p,mn}^x(x, y, z) \end{aligned} \tag{6a}$$

$$\begin{aligned} E_y(\vec{r}) &= \sum_{m=1}^{\infty}\sum_{n=1}^{\infty}\Big[\Big(I_{1,mn}^ye_{mn}^{(2)} + I_{2,mn}^ye_{mn}^{(1)} + I_{3,mn}^ye_{mn}^{(4)}\Big) \cdot \cos k_{z,mn}z + \Big(I_{4,mn}^ye_{mn}^{(2)} + I_{5,mn}^ye_{mn}^{(1)} + I_{6,mn}^ye_{mn}^{(4)}\Big) \cdot \sin k_{z,mn}z\Big] \\ &= \sum_{m=1}^{\infty}\sum_{n=1}^{\infty}\sum_{p=1}^{6} I_{p,mn}^yb_{p,mn}^y(x, y, z), \end{aligned} \tag{6b}$$

$$\begin{aligned} E_z(\vec{r}) &= \sum_{m=1}^{\infty}\sum_{n=1}^{\infty}\Big[\Big(I_{1,mn}^ze_{mn}^{(3)} + I_{2,mn}^ze_{mn}^{(4)} + I_{3,mn}^ze_{mn}^{(1)}\Big) \cdot \cos k_{z,mn}z + \Big(I_{4,mn}^ze_{mn}^{(3)} + I_{5,mn}^ze_{mn}^{(4)} + I_{6,mn}^ze_{mn}^{(1)}\Big) \cdot \sin k_{z,mn}z\Big] \\ &= \sum_{m=1}^{\infty}\sum_{n=1}^{\infty}\sum_{p=1}^{6} I_{p,mn}^zb_{p,mn}^z(x, y, z), \end{aligned} \tag{6c}$$

where

$$e_{mn}^{(1)} = \sin\left(\frac{m\pi}{2W}x\right)\sin\left(\frac{n\pi}{2L}y\right)$$
$$e_{mn}^{(2)} = \cos\left(\frac{m\pi}{2W}x\right)\cos\left(\frac{n\pi}{2L}y\right)$$
$$e_{mn}^{(3)} = \cos\left(\frac{m\pi}{2W}x\right)\sin\left(\frac{n\pi}{2L}y\right)$$
$$e_{mn}^{(4)} = \sin\left(\frac{m\pi}{2W}x\right)\cos\left(\frac{n\pi}{2L}y\right)$$
$$k_{z,mn} = \left[\varepsilon_r k_o^2 - \left(\frac{m\pi}{2W}\right)^2 - \left(\frac{n\pi}{2L}\right)^2\right]^{1/2}$$

and

$$I_{p,mn}^q (q = x, y, z)$$

are the unknown coefficients of the electric field inside the DR. $I_{1,mn}^z e_{mn}^{(3)} \cos k_{z,mn} z$ and $I_{4,mn}^z e_{mn}^{(3)} \sin k_{z,mn} z$ in (6c) dominate the electric field E_z inside the DR at the resonance of the TE_{111}^x mode. Similarly, $I_{2,mn}^z e_{mn}^{(4)} \cos k_{z,mn} z$, $I_{5,mn}^z e_{mn}^{(4)} \sin k_{z,mn} z$, $I_{3,mn}^z e_{mn}^{(1)} \cos k_{z,mn} z$, and $I_{6,mn}^z e_{mn}^{(1)} \sin k_{z,mn} z$ in (6c) dominate the electric field E_z inside the DR at the resonance of TE_{111}^y and TE_{111}^z modes, respectively. Here, the mode nomenclature follows the definition by Mongia and Ittipiboon [9]. If the dimensions of an isolated DR are such that $2W > 2L > 2h$, the modes in the order of increasing resonant frequency are TE_{111}^z, TE_{111}^y, and TE_{111}^x.

Next, substituting the Fourier transforms of (6) into (2), then applying the Galerkin's moment method, and integrating (2) over the rectangular dielectric volume, we have the following matrix equation:

$$\sum_{m=1}^{\infty}\sum_{n=1}^{\infty}\int_{-\infty}^{\infty}\int_{-\infty}^{\infty} dk_x dk_y \left[\int_{z_b}^{z_t} dz \overline{\overline{w}}(k_x, k_y, z)\overline{\overline{S}}\,\overline{\overline{\tilde{b}}}^T(k_x, k_y, z) + \frac{j(\varepsilon_r - 1)}{2}\int_{z_b}^{z_t}\int_{z_b}^{z_t} dz dz' \overline{\overline{w}}(k_x, k_y, z) \cdot \frac{\overline{\overline{g}}(k_x, k_y; z, z')}{k_z}\overline{\overline{\tilde{b}}}^T(k_x, k_y, z')\right] = 0 \tag{7}$$

with

$$\overline{\overline{w}}(k_x, k_y, z) = \begin{bmatrix} \sum_{p=1}^{6} \tilde{b}_{p,mn}^x(-k_x, -k_y, z) \\ \sum_{p=1}^{6} \tilde{b}_{p,mn}^y(-k_x, -k_y, z) \\ \sum_{p=1}^{6} \tilde{b}_{p,mn}^z(-k_x, -k_y, z) \end{bmatrix}$$

$$\overline{\overline{\tilde{b}}}(k_x, k_y, z) = \begin{bmatrix} \sum_{p=1}^{6} I_{p,mn}^x \tilde{b}_{p,mn}^x(k_x, k_y, z) \\ \sum_{p=1}^{6} I_{p,mn}^y \tilde{b}_{p,mn}^y(k_x, k_y, z) \\ \sum_{p=1}^{6} I_{p,mn}^z \tilde{b}_{p,mn}^z(k_x, k_y, z) \end{bmatrix}$$

$$\overline{\overline{S}} = \begin{bmatrix} 1 & 0 & 0 \\ 0 & 1 & 0 \\ 0 & 0 & \varepsilon_r \end{bmatrix}$$

where the superscript T denotes a matrix transpose and z_t and z_b are the z-directional positions that correspond to the top surface and bottom surfaces of the DR, respectively. $\tilde{b}_{p,mn}^q(k_x, k_y, z)$ is the two-dimensional Fourier transfrom of $b_{p,mn}^q(x, y, z)$; $q = x, y, z$.

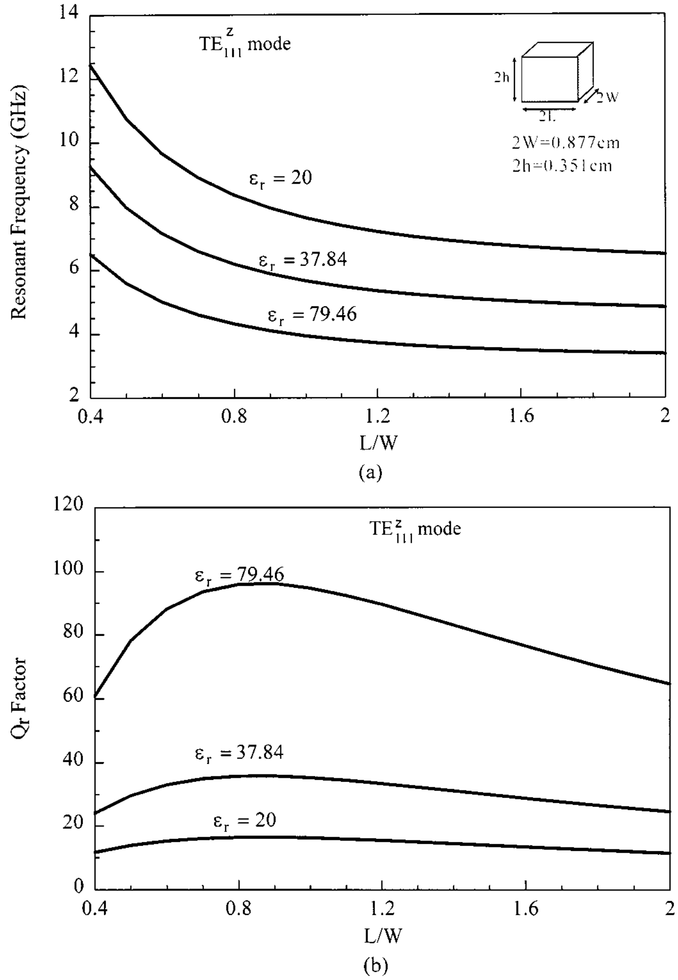

Fig. 2. Resonant frequencies and Q_r factors of the TE_{111}^z modes versus the aspect ratios (L/w) for isolated rectangular DRs: $2W = 0.877$ cm, $2h = 0.351$ cm $\varepsilon_r = 20$, 37.84, and 79.46. (a) Resonant frequencies. (b) Q_r factors.

In (7), the integration along z- and z'-directions can be derived as analytical expressions, which, for brevity, are not included in this paper. Thus, the three-dimensional integral equations in (7) can be transferred into two-dimensional integral problems. Finally, (7) is rewritten as a general matrix form in the moment method

$$\overline{\overline{Z}}_{N\times N}\overline{\overline{I}}_N = 0 \tag{8}$$

where $\overline{\overline{Z}}_{N\times N}$ is the impedance matrix whose elements are electric-field integration equations defined in (7), $\overline{\overline{I}}_N$ is a column matrix whose elements correspond to the unknown coefficient $I_{p,mn}^q$ in (6). Equation (8) has a nontrivial solution for $\overline{\overline{I}}_N$ if the determinant of $\overline{\overline{Z}}_{N\times N}$ vanishes. This condition is satisfied by complex resonant frequencies, i.e.,

$$\det\left(\overline{\overline{Z}}_{N\times N}\right)\Big|_{f=f_r+jf_i} = 0 \tag{9}$$

where f_r and f_i are, respectively, the real part and imaginary parts of the complex resonant frequency. For a particular resonant mode of a DR with real permittivity, f_r gives the resonant frequency and $Q_r(= f_r/(2f_i))$ gives the radiation Q factor of the DR.

III. Results and Discussions

In this section, two cases for open rectangular DRs in typical microwave applications are investigated. As shown in Fig. 1, they are the

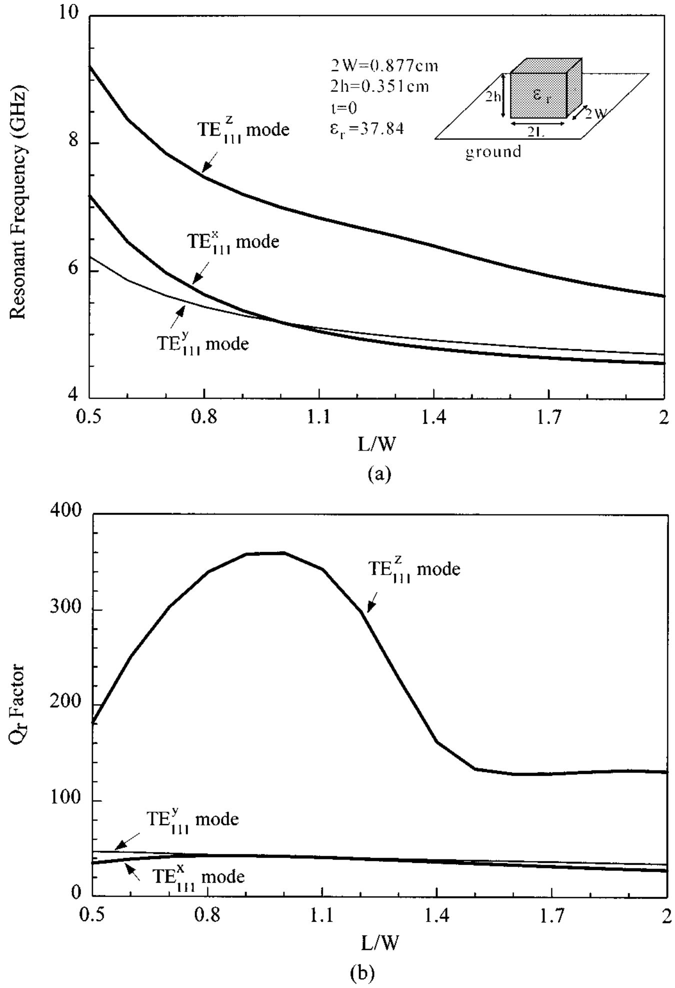

Fig. 3. Variations of resonant frequencies and Q_r factors with the aspect ratios (L/W) for grounded rectangular DRs excited at TE^x_{111}, TE^y_{111}, and TE^z_{111} modes: $2W = 0.877$ cm, $2h = 0.351$ cm, $\varepsilon_r =$ 37.84. (a) Resonant frequencies. (b) Q_r factors.

isolated DR (in the absence of the grounded substrate) and the DR on a ground plane (the substrate thickness is zero). In the calculation of the moment method, nine bases ($m = 1,\ n = 1,\ p = 1,\ 2,\ 3$) and 18 bases ($m = 1,\ n = 1,\ p = 1,\ 2,\ 3,\ 4,\ 5,\ 6$) are, respectively, chosen for the isolated DR and the DR on a ground plane. Since the integrand in (7) has branch points and poles, the integration path in our numerical computation is selected to be the deforming contour in the β-plane [10]. Such an integration path can avoid the numerical error due to singularities existing in the integrand [7]. The required CPU time for computing the complex frequencies of an isolated DR and a DR on a grounded plane are, respectively, about 6 and 22 min on a Pentium-333 PC. The discrepancy between the theoretical resonant frequencies and the experimental resonant frequencies [9] is within 0.6% for the isolated DR cases.

The effects of electrical and geometrical parameters on the resonance of the TE^z_{111} mode for isolated rectangular DRs are presented in Fig. 2. It can be seen that the rectangular DRs with lower permittivity have lower Q_r factor (higher radiation loss). Besides, the dimension of a rectangular DR also affects its Q_r factor. This is due to the fact that the geometry factor confines the degree of field concentration in the rectangular DR [4]. Next, numerical results for the effects of the ground plane on the resonance of the TE_{111} mode are shown in Fig. 3. Comparing Fig. 3 with Fig. 2, it can be found that the Q_r factor of the TE^z_{111} mode of a rectangular DR on a ground plane is much higher than that of the isolated rectangular DR case. Thus, a high-permittivity grounded rectangular DR excited at the TE^z_{111} mode is suitable for using as a filter (or a resonator) under adequate aspect ratio (e.g., $L/W \cong 1$) conditions. On the contrary, the grounded rectangular DR excited at the TE^x_{111} or TE^y_{111} modes is better for using as an antenna since it has lower Q_r factors. It should be noted that the resonant frequency and Q_r factor of the TE^x_{111} mode are the same as those of the TE^y_{111} mode at $W = L$. That is, degenerate modes can also be excited in a rectangular DR structure. Furthermore, the behavior features of the Q_r factors strongly depend on the resonant modes of the DRs. The reason is the different radiation effects resulted from vertical magnetic dipoles (resonance in the TE^z_{111} mode) and horizontal magnetic dipoles (resonance in the TE^x_{111} or TE^y_{111} mode) above a ground plane [9].

IV. Conclusions

In this paper, the integral-equation approach has been employed to solve the resonance problems of open rectangular DR structures. It can be used to accurately calculate the complex resonant frequencies of rectangular DR structures, as discussed here. Besides, the entire-domain basis functions based on the magnetic wall model has been presented. The integral equation in conjunction with the sinusoidal basis functions is more efficient for computing the resonance problems of three-dimensional rectangular structures. Next, the numerical results show that a high-permittivity grounded DR excited at the TE^z_{111} mode is suitable for use as a filter or a resonator. On the other hand, the low-permittivity rectangular DR excited at the TE^x_{111} (or TE^y_{111}) mode is good for use as an antenna. Here, we conclude that the DRs permittivity together with geometrical factors should be considered in a rectangular DR antenna (or filter) design.

References

[1] D. Baillargeat, S. Verdeyme, M. Aubourg, and P. Guillon, "CAD applying the finite-element method for dielectric-resonator filters," *IEEE Trans Microwave Theory Tech.*, vol. 46, pp. 10–17, Dec. 1998.

[2] C. Y. Hung, J. Y. Wu, and K. L. Wong, "Cross-slot-coupled microstrip antenna and dielectric resonator antenna for circular polarization," *IEEE Trans. Antennas Propagat.*, vol. 47, pp. 605–609, Apr. 1999.

[3] A. W. Glisson, D. Kajfez, and J. James, "Evaluation of modes in dielectric resonators using a surface integral formulation," *IEEE Trans. Microwave Theory Tech.*, vol. MTT-31, pp. 1023–1029, Dec. 1983.

[4] M. Tsuji, H. Shigesawa, H. Aoki, and K. Takiyama, "Analytical and experimental considerations on the resonant frequency and the quality factor of dielectric resonators," *IEEE Trans. Microwave Theory Tech.*, vol. MTT-30, pp. 1952–1957, Nov. 1982.

[5] K. A. Zaki and C. Chen, "Loss mechanisms in dielectric-loaded resonators," *IEEE Trans. Microwave Theory Tech.*, vol. MTT-33, pp. 1448–1452, Dec. 1985.

[6] J. A. Pereda, L. A. Vielva, A. Vegas, and A. Prieto, "Computation of resonant frequencies and quality factors of open dielectric resonators by a combination of the finite-difference time-domain (FDTD) and Prony's Method," *IEEE Microwave Guided Wave Lett.*, vol. 2, pp. 431–433, Nov. 1992.

[7] W. C. Chew, *Waves and Fields in Inhomogeneous Media*. New York: Van Nostrand, 1990.

[8] S. T. Peng and A. A. Oliner, "Guidance and leakage properties of a class of open dielectric waveguides—Part I: Mathematical formulations," *IEEE Trans. Microwave Theory Tech.*, vol. MTT-29, pp. 843–855, Sept. 1981.

[9] R. K. Mongia and A. Ittipiboon, "Theoretical and experimental investigations on rectangular dielectric resonator antennas," *IEEE Trans. Antennas Propagat.*, vol. 45, pp. 1348–1355, Apr. 1997.

[10] J. S. Row and K. L. Wong, "Resonance in a superstrate-loaded rectangular microstrip antenna," *IEEE Trans. Microwave Theory Tech.*, vol. 41, pp. 1349–1355, Aug. 1993.